

## Electrical Pulses To Determine Chemical Phase Response Curves

G. Dechert, D. Lebender, and F. W. Schneider\*

Institut für Physikalische Chemie, Universität Würzburg, Marcusstrasse 9-11, D-97070 Würzburg, Germany

Received: March 10, 1995; In Final Form: May 17, 1995<sup>⊗</sup>

We report several series of single perturbation experiments in the Belousov–Zhabotinsky (BZ) reaction which have been carried out by applying an electrical current to a platinum electrode in the continuous flow stirred tank reactor (6.4 mL). When a single short current pulse is applied at the maximum of a chemical oscillation (high  $\text{Ce}^{4+}$  concentration) or at the minimum (low  $\text{Ce}^{4+}$ ), the response is a small advance or a significant delay of the original phase of oscillation (negative or positive phase shift), respectively. Thus we obtain phase response curves as a function of electrical current strength and duration of the pulses. These results show that the redox reactions occurring at the platinum electrodes involve mainly the  $\text{Ce}^{3+}/\text{Ce}^{4+}$  redox couple as supported by pulsed additions of known  $\text{Ce}^{4+}$  solutions. Numerical simulations are in good agreement with the experiments.

### Introduction

Coupled oscillators of identical frequencies may store information by arranging their phases in a non-statistical manner.<sup>1</sup> In order to set a specific phase difference between two oscillators it is necessary to apply short perturbations at certain times during the cycle. This is accomplished on the basis of the phase response curve (PRC) of the oscillator. PRCs of chemical oscillators have been measured by pulsed injections of chemical species in many instances. PRCs have been determined in biological<sup>2</sup> and in nonbiological systems such as the Briggs–Rauscher reaction;<sup>3</sup> for an earlier review see ref 4. In the Belousov–Zhabotinsky (BZ) reaction, Vavilin et al.<sup>5</sup> used phase shift experiments by pulsed injections of  $\text{Br}^-$ ,  $\text{Ag}^+$ , and  $\text{Ce}^{4+}$  ions to determine the role of  $\text{Br}^-$  in the mechanism. Marek and co-workers<sup>6–9</sup> and Ruoff et al.<sup>10–12</sup> further investigated the PRCs of these and other perturbants in the BZ reaction. Sørensen and co-workers<sup>13–15</sup> quenched limit cycle oscillations near a supercritical Hopf bifurcation by injections of  $\text{Br}^-$ ,  $\text{HBrO}_2$ , or  $\text{Ce}^{4+}$  solutions to obtain quantitative information about the dynamics of the BZ reaction. In this work we describe a novel way of determining a PRC of a chemical oscillator, namely by the application of a single electric current pulse at various phases of the unperturbed cycle. We employ the well-defined period one oscillations of the BZ reaction. Perturbations with additions of  $\text{Ce}^{4+}$  solutions will be used as a comparison. All resulting PRCs are simulated with the seven-variables model of Györgyi and Field.<sup>16–18</sup> It is expected that electrical current perturbations are more efficient and less invasive than additions of solutions of reactive species. Electrical current pulses will always perturb a chemical oscillator, if the mechanism contains redox processes.

### The Phase Response Curves

The response behavior of oscillations toward single perturbations can be interpreted as PRCs<sup>11</sup> or phase transition curves (PTC).<sup>19</sup> Figure 1 displays a measured limit cycle oscillation. The dashed curve represents the unperturbed oscillation, whereas the bold curve displays the positive phase shift (phase delay) after a pulse perturbation has been applied at the minimum of the oscillation. The original period  $P_0$  is defined as usual (Figure

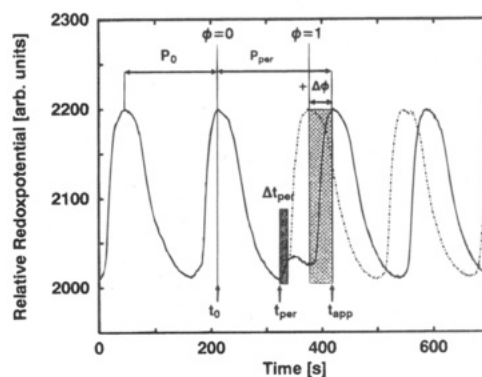


**Figure 1.** Single perturbation experiment of a  $P_1$  oscillation (dotted curve) of period  $P_0$  at  $t_{\text{per}}$  induced by an electrical current of duration  $\Delta t_{\text{per}}$ . The phase response behavior shows a positive phase shift  $\Delta\phi$  of the perturbed limit cycle oscillation (solid curve) that indicates a retarded oscillation with period  $P_{\text{per}}$  relative to  $P_0$ . The appearance of a single small maximum is a consequence of the momentary  $\text{Ce}^{4+}$  produced by the pulsed anodic current.

2). At  $t_{\text{per}}$  the oscillation is perturbed by a pulsed electrical current of pulse length  $\Delta t_{\text{per}}$  where the duration of the perturbation is short compared with  $P_0$  (i.e.,  $\Delta t_{\text{per}} < 0.1 P_0$ ). After the perturbation, the next  $\text{Ce}^{4+}$  maximum appears at  $t_{\text{app}}$  and the perturbed period  $P_{\text{per}}$  is the time between the preceding  $\text{Ce}^{4+}$  maximum at  $t_0$  and the perturbed maximum at  $t_{\text{app}}$ . If  $P_{\text{per}}$  is different from  $P_0$ , one observes a finite phase shift  $\Delta\phi$  (normalized to  $P_0$ ):

$$\Delta\phi = (P_{\text{per}} - P_0)/P_0 \quad (1)$$

A phase delay (retardation) is called a positive phase shift,  $\Delta\phi > 0$ , while a phase advance,  $\Delta\phi < 0$ , is termed a negative phase shift. We arbitrarily assign the value  $\phi = 0$  to the maximum ( $t_0$ ) of the chemical oscillation. The phase  $\phi$  at which the perturbation is applied is defined by

$$\phi = (t_{\text{per}} - t_0)/P_0 \quad (2)$$

The minimum of  $\text{Ce}^{4+}$  occurs at  $\phi = 0.72–0.75$  (Figure 1) in the experiment and in the simulation. The PRC is a plot of the phase shift  $\Delta\phi$  versus  $\phi$  (Figures 3–7). Figure 2 shows an unperturbed oscillation (grey area) of  $P_0$ . The box (inset) is a measured PRC which shows that the maximum in the phase

\* To whom correspondence should be addressed.

<sup>⊗</sup> Abstract published in *Advance ACS Abstracts*, July 1, 1995.

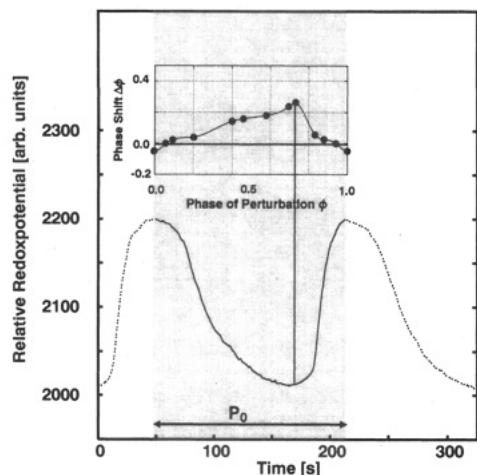


**Figure 2.** A phase response curve (inset) showing the greatest positive phase shift when the perturbation occurs either by electrical current or by  $\text{Ce}^{4+}$  solutions at the minimum of the oscillator (lowest  $\text{Ce}^{4+}$  concentration). When the perturbation is applied at the maximum of the oscillation (high  $\text{Ce}^{4+}$  concentration) a small negative phase shift occurs.

**TABLE 1: Seven-Variables Model (Nonstoichiometric Steps)<sup>a</sup>**

$\text{HBrO}_2 + \text{Br}^- + \text{H}^+ \rightarrow 2\text{BrMA}$	S1
$\text{BrO}_3^- + \text{Br}^- + 2\text{H}^+ \rightarrow \text{HBrO}_2 + \text{BrMA}$	S2
$2\text{HBrO}_2 \rightarrow \text{BrO}_3^- + \text{BrMA} + \text{H}^+$	S3
$\text{BrO}_3^- + \text{HBrO}_2 + \text{H}^+ \rightleftharpoons 2\text{BrO}_2^* + \text{H}_2\text{O}$	S4/S5
$\text{Ce}^{3+} + \text{BrO}_2^* + \text{H}^+ \rightleftharpoons \text{HBrO}_2 + \text{Ce}^{4+}$	S6/S7
$\text{MA} + \text{Ce}^{4+} \rightarrow \text{MA}^* + \text{Ce}^{3+} + \text{H}^+$	S8
$\text{BrMA} + \text{Ce}^{4+} \rightarrow \text{Ce}^{3+} + \text{Br}^-$	S9
$\text{MA}^* + \text{BrMA} \rightarrow \text{MA} + \text{Br}^-$	S10
$2\text{MA}^* \rightarrow \text{MA}$	S11

<sup>a</sup> MA = malonic acid; MA\* = malonic acid radical; BrMA = bromomalonic acid.

shift occurs at the minimum of the  $\text{Ce}^{4+}$  concentration. Small negative phase shifts are observed close to the maximum of the unperturbed  $\text{Ce}^{4+}$  concentration. The electrical pulse perturbation is found to produce phase shifts only during one period.

### Experimental Setup

The experimental setup<sup>20</sup> consists of two electrically coupled continuous flow-stirred tank reactors (CSTRs), 6.4 mL each, which are separated by two permeable membranes (1–2  $\mu\text{m}$  pore size). A solution of 0.8 M  $\text{H}_2\text{SO}_4$  flows constantly between the two membranes to avoid mass exchange between the CSTRs. The reactors are equipped with Pt working electrodes (3.4  $\text{cm}^2$  surface) which are connected with a potentiostat supplying and regulating the single current pulses in strength as well as in time via a D/A channel of a personal computer. Potential changes are measured with Pt/Ag/AgCl reference electrodes and registered as described in refs 20 and 21. Due to the variations in the sensitivity of the commercial redox electrodes, we present the output in arbitrary units. Each reactor is fed by three reactant feed streams, delivered by a precise three-channel syringe pump. The feed streams enter through the bottom of the CSTRs. To obtain limit cycle oscillations with sufficiently long periods, the following reactor concentrations are used (Table 2): (a) 0.27 M  $\text{H}_2\text{SO}_4$ , (b) 0.047 M  $\text{KBrO}_3$ , and (c)  $3.3 \times 10^{-4}$  M  $\text{Ce}_2(\text{SO}_4)_3$  and 0.033 M malonic acid, which was recrystallized twice from acetone.<sup>22,23</sup> The other reactants were used without further purification. The experiments were carried out at  $25.0 \pm 0.2$  °C at a stirring rate of 600 rpm using magnetic stirrers. The flow rate was set to  $k_f = 3.77 \times 10^{-4}$   $\text{s}^{-1}$  (residence time  $\tau_{\text{res}}$

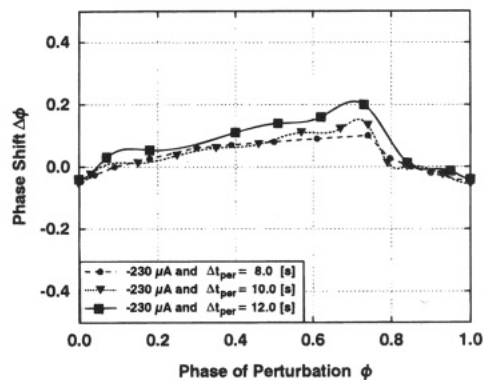


**Figure 3.** PRCs by electrical perturbations ( $-230 \mu\text{A}$ ) of different durations (see inset). Negative values of  $\Delta\phi$  indicate phase advances of the perturbed response whereas a positive  $\Delta\phi$  indicates a phase delay. Longer duration times  $\Delta t_{\text{per}}$  lead to larger phase shifts  $\Delta\phi$ .

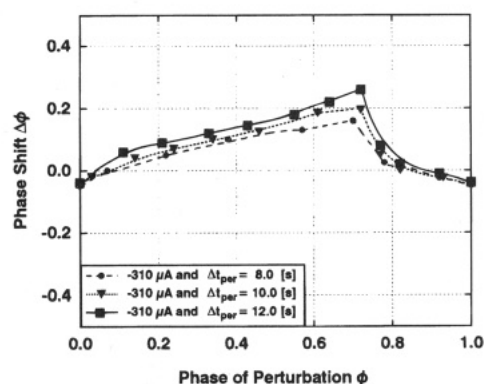


**Figure 4.** PRCs by short electrical perturbations ( $-310 \mu\text{A}$ ) of different durations (see inset). The phase shifts  $\Delta\phi$  are larger than those in Figure 2.

**TABLE 2: Rate Constants of the Seven-Variables Model and Reactor Concentrations (Experiment and Model)**

$k_{S1}$	$2.0 \times 10^6 \text{ s}^{-1} \text{ M}^{-2}$	$k_{S2}$	$2.0 \text{ s}^{-1} \text{ M}^{-3}$
$k_{S3}$	$3.0 \times 10^3 \text{ s}^{-1} \text{ M}^{-1}$	$k_{S4}$	$3.3 \times 10^1 \text{ s}^{-1} \text{ M}^{-2}$
$k_{S5}$	$7.6 \times 10^5 \text{ s}^{-1} \text{ M}^{-2}$	$k_{S6}$	$6.2 \times 10^4 \text{ s}^{-1} \text{ M}^{-2}$
$k_{S7}$	$7.0 \times 10^3 \text{ s}^{-1} \text{ M}^{-1}$	$k_{S8}$	$3.0 \times 10^{-1} \text{ s}^{-1} \text{ M}^{-1}$
$k_{S9}$	$3.0 \times 10^1 \text{ s}^{-1} \text{ M}^{-1}$	$k_{S10}$	$2.4 \times 10^4 \text{ s}^{-1} \text{ M}^{-1}$
$k_{S11}$	$3.0 \times 10^9 \text{ s}^{-1} \text{ M}^{-1}$		
[MA]	0.033 M	[H <sup>+</sup> ]	0.27 M
[Ce <sup>3+</sup> ]	$3.3 \times 10^{-4}$ M	[BrO <sub>3</sub> <sup>-</sup> ]	0.047 M

= 44.2 min), where the BZ reaction oscillates in a period-1 state with  $P_1 = 168 \pm 1$  s.

### Results

**Single-Pulse Experiments.** PRCs obtained by an applied current are shown in Figures 3–5 or by perturbation with a  $\text{Ce}^{4+}$  solution in Figure 6. The electrical perturbations (Figures 3–5) were applied with three different anodic currents ( $-230$ ,  $-310$ , and  $-430 \mu\text{A}$ ), each with three different pulse lengths (8, 10, and 12 s) measured below 1.1 V. The range of variation of the current strength was chosen in order to keep the potential below the  $[\text{Ce}^{3+}/\text{Ce}^{4+}]$  standard redox potential (1.44 V).<sup>24</sup> Care was taken to produce only perturbations of less than 10% of the period of the limit cycle oscillations. No significant phase shifts for single anodic current perturbations were observed when the current was below  $-200 \mu\text{A}$  with a pulse length of less than 8 s. For the given current parameters, a perturbation applied at  $\phi = 0$  causes a phase advance of about  $-0.04$  ( $P_{\text{per}} = 160$ – $161$  s), approximately independent of the applied current. The response behavior turns into a positive phase shift and increases until the  $\text{Ce}^{4+}$  concentration reaches a minimum.

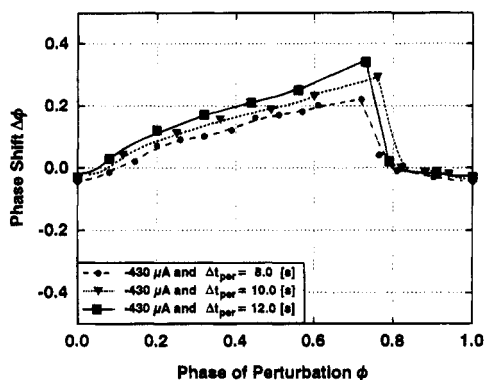


**Figure 5.** PRCs by short electrical perturbations ( $-430 \mu\text{A}$ ) of different durations (see inset).

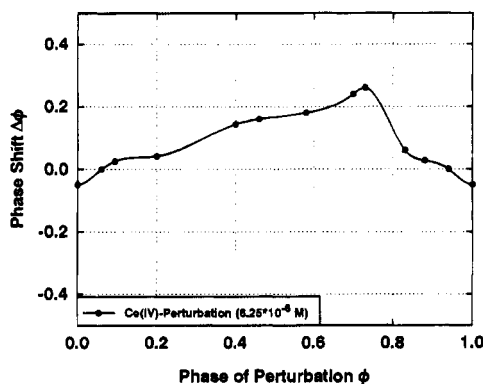


**Figure 6.** PRCs obtained by the pulsed addition of  $10 \mu\text{L}$  of  $\text{Ce}^{4+}$  solution ( $[\text{Ce}^{4+}]_0 = 4.0 \times 10^{-3} \text{ M}$ ) into the CSTR ( $6.4 \text{ mL}$ ).

The above phase retardation depends on the phase ( $\phi \approx 0.08 - 0.75$ ), the strength, and the duration of the applied current perturbation.  $\Delta\phi$  increases almost linearly with current strength and duration, while  $\phi$  approaches the lowest values of the  $\text{Ce}^{4+}$  concentration. The highest positive phase shifts are reached between  $\phi = 0.72$  and  $\phi = 0.75$ .  $\Delta\phi$  runs from  $0.1$  ( $-2.30 \mu\text{A}$  and  $8 \text{ s}$ ) to  $0.34$  ( $-430 \mu\text{A}$  and  $12 \text{ s}$ ), which corresponds to a phase delay from  $170$  to  $226 \text{ s}$  of the perturbed phase at  $\phi = 0.75$ . At  $\phi \approx 0.75$  the positive phase shift sharply decreases to zero and becomes negative. Generally speaking, the shape of the phase response curve is relatively smooth only at a low amplitude of the applied current (Figure 3) at  $\phi \approx 0.75$ . At high current amplitudes (Figures 4 and 5) the phase response curves show relatively sharp changes from positive to negative values of  $\Delta\phi$ . A similar behavior has also been observed in the Briggs–Rauscher reaction<sup>3</sup> when the perturbation was carried out by the addition of a  $\text{Br}^-$  solution.

The above phase response behavior was only observed for the anodic current. Experiments with cathodic current in the same parameter ranges do not show any detectable phase shifts. To prove the assumption that the oxidation of  $\text{Ce}^{3+}$  to  $\text{Ce}^{4+}$  is responsible for the observed behavior, we measured a phase response curve with a  $\text{Ce}^{4+}$  solution as the perturbing agent. Figure 6 shows the measured PRC obtained by perturbations with  $6.25 \times 10^{-6} \text{ M}$   $\text{Ce}^{4+}$ . The response behavior is identical to the anodic current perturbations, if we assume that the oxidation of  $\text{Ce}^{3+}$  to  $\text{Ce}^{4+}$  is the only oxidation process taking place at the electrode. Measurements with  $\text{Ce}^{3+}$  solutions of various concentrations, as well as injection experiments with the solvent<sup>7</sup> at different phases yielded neither a phase delay nor a phase advance. Thus we conclude that the observed behavior is sensitive only towards  $\text{Ce}^{4+}$ .

**Simulations.** For the numerical simulations of the observed phase response behavior we used the seven-variable model for

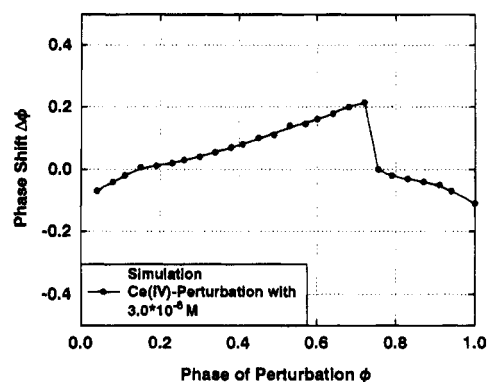


**Figure 7.** Simulation of a PRC by an "electrical"  $\text{Ce}^{4+}$  perturbation, where  $\phi = 0$  refers to the maximum of the oscillation.

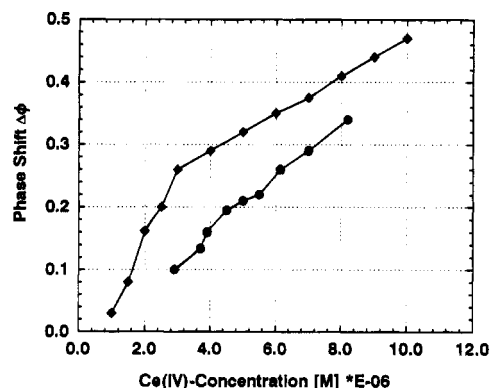


**Figure 8.** Phase shifts  $\Delta\phi$  versus  $\text{Ce}^{4+}$  concentrations of the perturbation measured at the minimum of the oscillation ( $\phi = 0.75$ ). The squares show the results of simulated perturbations. The circles are calculated from the experimentally measured current strength and duration.

the BZ reaction proposed by Györgyi and Field.<sup>16–18</sup> The chemical reactions, which are considered in this mechanism are given in Table 1. In our simulations, we employed the same concentrations and the same flow rate as in the experiments (Table 2). In this parameter range the model shows slow limit cycle oscillations. The mass balance of the cerium ions was kept constant throughout the numerical perturbing process. The result of a  $\text{Ce}^{4+}$  perturbation with  $3.0 \times 10^{-6} \text{ M}$  is shown in Figure 7. We find an almost linear increase of the phase delay up to  $\phi = 0.72$ . Here the phase shift sharply declines to negative values until the next  $\text{Ce}^{4+}$  maximum in the oscillation cycle is reached at  $\phi = 0$ . Thus the numerical simulations are in good agreement with the experiments.

Figure 8 displays simulated and measured phase shifts obtained by a perturbation applied at the minimum of the oscillation ( $\phi = 0.75$ ) as a function of the concentration of the  $\text{Ce}^{4+}$  perturbant. In the experiment the  $\text{Ce}^{4+}$  concentrations resulting from the redox process  $\text{Ce}^{3+} \rightarrow \text{Ce}^{4+}$  (circles in Figure 8) are calculated from the applied current as

$$[\text{Ce}^{4+}] = \frac{I\Delta t_{\text{per}}}{FV_{\text{CSTR}}}[\text{M}] \quad (3)$$

where  $I$  is the current in amperes,  $F$  is Faraday's constant ( $=96485 \text{ C mol}^{-1}$ ), and  $V_{\text{CSTR}}$  represents the volume of the CSTR. In the experiments as well as in the simulations (Figure 8, squares) the induced phase shift increases almost linearly with increasing  $\text{Ce}^{4+}$  concentration. There is a systematic shift between experiments and simulations of the order of  $\Delta\text{Ce}^{4+} \approx 1.5 \times 10^{-6} \text{ M}$ , which is an expression of the simplifications inherent in the seven-variables model.

## Discussion

The BZ oscillations in the chosen parameter range are represented as relaxation oscillations between two dynamic states. The first state is characterized by low  $Ce^{4+}$  and high bromide concentrations. Bromate reacts with malonic acid to produce bromomalonic acid with bromous acid as an intermediate (reaction S2 and S1, Table 1). The second dynamic state is reached at high  $Ce^{4+}$  (low bromide) concentrations. In this case the bromate is reduced in an autocatalytic cycle with bromous acid as the autocatalytic species (reactions S2, S4–S7, Table 1). Relaxation oscillations are obtained as continuous transitions between these two states: Reduction of bromate along the first pathway consumes bromide until its concentration falls below a critical volume. Then the autocatalytic pathway of reduction is initiated. While the reduction of bromate takes place via this autocatalytic route,  $Ce^{4+}$  is produced (reaction S6, Table 1) which releases bromide from the brominated organic species (reaction S9, Table 1). Therefore, the concentration of bromide increases and the dynamic behavior switches back to the state determined by the first, nonautocatalytic state.<sup>4,10</sup> A possible explanation of the experimentally observed phase shifts may be as follows: An electrochemical oxidation on the surface of the Pt electrode is postulated which includes the transfer of a single electron. The radicals  $BrO_2^*$  and  $MA^*$  as well as the  $Ce^{3+}$  ions are likely candidates for oxidation at the electrode. According to Field and Försterling,<sup>25</sup> bromate and bromous acid form a homogeneous equilibrium with the bromide dioxide radical (S4, S5, Table 1). The removal of the bromide dioxide through an electrochemical process at the electrode would cause the bromide dioxide to be resupplied according to the equilibrium constant. Therefore, an appreciable kinetic effect on the overall dynamic behavior of the BZ reaction would not be expected. The concentrations of the malonyl radical ( $\approx 5.0 \times 10^{-9}$  M) are too low to explain the relatively large electric current measured at the Pt electrode. An absolute conversion of electrons at the Pt electrode corresponds to  $3.0 \times 10^{-6}$  M converted species at  $-230 \mu A$  and  $9.0 \times 10^{-6}$  M at  $-430 \mu A$ . The only process remaining to explain the effective electrical current is the anodic oxidation of  $Ce^{3+}$  where only  $\sim 1\%$  of the  $Ce^{3+}$  is oxidized to  $Ce^{4+}$ , which releases bromide from the organic components of the BZ reaction via reaction S9 (Table 1).

At low  $Ce^{4+}$  concentrations, the bromide concentration is high and it will be slowly consumed by reaction S1 (Table 1). Anodic oxidation of  $Ce^{3+}$  to  $Ce^{4+}$  causes an increase in bromide concentration by reaction S9 such that the state with high bromide concentrations prevails for a longer time. Hence, the phase of the oscillation may be shifted.

On the other hand, the bromide concentration is low if the system stays at high  $Ce^{4+}$  concentrations. The electrochemical oxidation of  $Ce^{3+}$  to  $Ce^{4+}$  sufficiently raises the bromide concentration and the system switches to the state characterized by high  $Br^-$  concentrations. Therefore, an applied electrical current advances the oscillation period.

A comparison between the phase response curves obtained from electrical current pulses and from  $Ce^{4+}$  solutions shows

that  $Ce^{4+}$  is likely to be the main product at the electrode. The  $Ce^{4+}$  produced at the electrode influences the phase response behavior of the BZ system as also shown by the PRC obtained from the addition of a  $Ce^{4+}$  solution (Figure 6). The phase shifts take place promptly within the same period after an electrical current has been applied. The magnitude of the phase shift can be regulated more sensitively with the current strength and the duration of the applied electrical current pulses than by injections of perturbant solutions which may lead to undesirable dilution effects. Flow rate changes also lead to slow dynamic responses which influence all species. The sum of all redox species of a given kind is always constant for electrical perturbations which simplifies the calculations. Thus electrical perturbations provide an excellent tool for sensitively and promptly adjusting the phase in an oscillating reaction in which redox processes are important. The analogies to biological systems are currently elaborated.

**Acknowledgment.** We thank the Deutsche Forschungsgemeinschaft and the Fonds der Chemischen Industrie for financial support of this work. We thank K. P. W. Zeyer, A. F. Münster, and M. J. B. Hauser for useful discussions.

## References and Notes

- (1) Gray, C. M.; König, P.; Engel, A. K.; Singer, W. *Nature* **1989**, *338*, 334.
- (2) Winfree, W. *The Geometry of Biological Time*; Springer Verlag: New York, 1980.
- (3) Dulos, P.; De Kepper, P. *Biophys. Chem.* **1983**, *211*, 18.
- (4) Schneider, F. W. *Annu. Rev. Phys. Chem.* **1985**, *36*, 347.
- (5) Vavilin, V. A.; Zhabotinsky, A. M.; Zaikin, A. N. In *Biological and Biochemical Oscillators*; Chance, B., Pye, E. K., Eds.; Academic Press: New York, 1973, p 71.
- (6) Dolník, M.; Padosáková, E.; Marek, M. *J. Phys. Chem.* **1987**, *91*, 4407.
- (7) Dolník, M.; Marek, M. *J. Phys. Chem.* **1988**, *92*, 2452.
- (8) Dolník, M.; Finkeová, J.; Schreiber, I.; Marek, M. *J. Phys. Chem.* **1989**, *93*, 2764.
- (9) Finkeová, J.; Dolník, M.; Hrudka, B.; Marek, M. *J. Phys. Chem.* **1990**, *94*, 4110.
- (10) Ruoff, P. *J. Phys. Chem.*, **1984**, *88*, 2851.
- (11) Ruoff, P.; Noyes, R. M. *J. Chem. Phys.* **1988**, *89*, 6247.
- (12) Ruoff, P.; Försterling, H.-D.; Györgyi, L.; Noyes, R. M. *J. Phys. Chem.* **1991**, *95*, 9314.
- (13) Hynne, F.; Sørensen, P. G. *J. Phys. Chem.* **1987**, *91*, 6573.
- (14) Sørensen, P. G.; Hynne, F. *J. Phys. Chem.* **1989**, *93*, 5467.
- (15) Nielsen, K.; Hynne, F.; Sørensen, P. G. *J. Chem. Phys.* **1991**, *94*, 1020.
- (16) Györgyi, L.; Field, R. J. *J. Phys. Chem.* **1991**, *95*, 6594.
- (17) Györgyi, L.; Field, R. J.; Rempe, S. L. *J. Phys. Chem.* **1991**, *95*, 3159.
- (18) Györgyi, L.; Field, R. J. *Nature* **1992**, *355*, 808.
- (19) Dolník, M.; Schreiber, I.; Marek, M. *Physica* **1986**, *21D*, 78.
- (20) Dechert, G.; Schneider, F. W. *J. Phys. Chem.* **1994**, *98*, 3927.
- (21) Zeyer, K.-P. W.; Dechert, G.; Hohmann, W.; Blittersdorf, R.; Schneider, F. W. *Z. Naturforsch.* **1994**, *49a*, 953.
- (22) Noszticzius, Z.; McCormick, W. D.; Swinney, H. L. *J. Phys. Chem.* **1987**, *91*, 5129.
- (23) Györgyi, L.; Field, R. J.; Noszticzius, Z.; McCormick, W. D.; Swinney, H. L. *J. Phys. Chem.* **1992**, *96*, 1228.
- (24) Vetter, K. J. *Z. Phys. Chem.* **1951**, *196*, 360.
- (25) Field, R. J.; Försterling, H.-D. *J. Phys. Chem.* **1986**, *90*, 5400.